Proc. Natl. Acad. Sci. USA
Vol. 93, pp. 9559–9564, September 1996
Cell Biology

Rab4 and cellubrevin define different early endosome populations on the pathway of transferrin receptor recycling

(endocytosis/recycling compartment/nocodazole/microtubules/brefeldin A)

ELIZABETH DARO*, PETER VAN DER SLUIJS†, THIERRY GALLI*, AND IRA MELLMAN*

*Department of Cell Biology, Yale University School of Medicine, New Haven, CT 06520-8002; and †Department of Cell Biology, Utrecht University School of Medicine, 3584 CX Utrecht, The Netherlands

Communicated by Vincent T. Marchesi, Yale University, New Haven, CT, May 15, 1996 (received for review April 11, 1996)

ABSTRACT **During receptor mediated endocytosis, at least a fraction of recycling cargo typically accumulates in a pericentriolar cluster of tubules and vesicles. However, it is not clear if these endosomal structures are biochemically distinct from the early endosomes from which they are derived. To better characterize this pericentriolar endosome population, we determined the distribution of two endogenous proteins known to be functionally involved in receptor recycling [Rab4, cellubrevin (Cbvn)] relative to the distribution of a recycling ligand [transferrin (Tfn)] as it traversed the endocytic pathway. Shortly after internalization, Tfn entered a population of early endosomes that contained both Rab4 and Cbvn, demonstrated by triple label immunofluorescence confocal microscopy. Tfn then accumulated in the pericentriolar cluster of recycling vesicles (RVs). However, although these pericentriolar endosomes contained Cbvn, they were strikingly depleted of Rab4. The ability of internalized Tfn to reach the Rab4-negative population was not blocked by nocodazole, although the characteristic pericentriolar location of the population was not maintained in the absence of microtubules. Similarly, Rab4-positive and -negative populations remained distinct in cells treated with brefeldin A, with only Rab4-positive elements exhibiting the extended tubular morphology induced by the drug. Thus, at least with respect to Rab4 distribution, the pathway of Tfn receptor recycling consists of at least two biochemically and functionally distinct populations of endosomes, a Rab4-positive population of early endosomes to which incoming Tfn is initially delivered and a Rab4-negative population of recycling vesicles that transiently accumulates Tfn on its route back to the plasma membrane.**

Receptor-mediated endocytosis is a process in which eukaryotic cells continuously internalize receptor-bound ligands together with other plasma membrane proteins and lipids, as well as extracellular solutes (reviewed in refs. 1 and 2). The basic features of the pathway are well understood and involve the internalization of receptor-ligand complexes via clathrin-coated pits to yield coated vesicles that rapidly lose their coats and fuse with a heterogeneous tubulovesicular network collectively referred to as early endosomes. Due in part to their acidic internal pH, early endosomes mediate the dissociation and then the sorting of receptors and ligands. Receptors appear to selectively accumulate in the early endosome's tubular extensions, which then bud off to yield a population of transport vesicles that mediate recycling back to the cell surface (3). Dissociated ligands, such as low density lipoprotein, are delivered to the late endosomes and lysosomes and are ultimately degraded. Transferrin (Tfn) undergoes a slightly more complicated cycle. Within early endosomes, Fe^{3+} dissociates from Tfn and the Tfn remains bound to its receptor (Tfn-R). The Tfn/Tfn-R complex then follows the recycling pathway back to the cell surface where the Tfn can reload with Fe^{3+} and repeat the cycle.

In many cells, at least a fraction of the vesicles that contain recycling cargo congregate in a distinctive perinuclear location, often in close apposition to the microtubule organizing center (MTOC) (4–8). These recycling vesicles (RVs) contain cargo that will be recycled back to the cell surface and lack cargo destined for late endosomes and lysosomes. Additionally, they are thought to have a pH less acidic than early or late endosomes and may allow for retention or retrograde transport of receptors back to early endosomes (6, 9, 10). Based on these observations, RVs are likely to represent a functionally distinct population of vesicles accessed after the early endosome-mediated sorting of recycling receptors from lysosomally directed components. However, RVs have thus far been distinguished only on the basis of itinerant cargo and their position in the cytoplasm. No resident marker proteins have been identified that define RVs in biochemical terms.

In recent years, a large number of small GTPases of the Rab family has been identified that serve critical regulatory roles in vesicular transport (11). Several Rab proteins are associated with the endocytic pathway. Rab4 and Rab5 colocalize with the Tfn-R in early endosomes, although not all Tfn-containing structures contain Rab4 or Rab5 (12, 13). Rab7 and Rab9 are associated with late endosomes (14, 15). While their precise functions are unknown, Rab4 and Rab5 control different aspects of transport through early endosomes. Rab5 potentiates lateral fusion between early endosomes *in vitro* and in intact cells may specify the fusion between endosomes and incoming coated vesicles (13, 16). In contrast, Rab4 is involved in a less well characterized event in the recycling of receptors back to the plasma membrane. Overexpression of Rab4 inhibits the discharge of iron from Tfn, apparently by mistargeting internalized Tfn to a population of non-acidic vesicles and tubules (12).

Endosomes are also known to be associated with at least one member of the SNARE family involved in vesicle docking and fusion (17, 18). This is the synaptobrevin/VAMP-related protein termed cellubrevin (Cbvn) (19). The Cbvn distribution overlaps with internalized Tfn, but its function and precise localization remain unknown. It clearly plays some important role since treatment of permeabilized CHO cells with tetanus toxin, a protease that cleaves synaptobrevin-like proteins, inhibits Tfn-R recycling (20).

To better characterize the pericentriolar clustering of RVs and to gain further understanding of Rab4 and Cbvn function, we examined the distribution of these two proteins relative to the distribution of a recycling ligand (Tfn) as it traversed the endocytic pathway. Strikingly, a subpopulation of MTOC-

The publication costs of this article were defrayed in part by page charge payment. This article must therefore be hereby marked "*advertisement*" in accordance with 18 U.S.C. §1734 solely to indicate this fact.

Abbreviations: Tfn, transferrin; Tfn-R, transferrin receptor; RVs, recycling vesicles; Cbvn, cellubrevin; FITC, fluorescein isothiocyanate; MTOC, microtubule organizing center; HA, hemagglutinin; BFA, brefeldin A.

associated RVs was found to have a distinctive membrane composition, being depleted in Rab4.

EXPERIMENTAL PROCEDURES

Cell Lines. The cells used in this study were CHO cells stably transfected with hemagglutinin (HA)-tagged human Rab4a and myc-human Tfn-R and will be described in detail elsewhere (P.v.d.S. and I.M., unpublished work). The cells were maintained in α-MEM containing 0.6 mg/ml of active G418. Prior to all experiments, expression of Rab4 and human (h)Tfn-R were induced by incubating cells for 15–18 hr in medium containing 10 mM sodium butyrate (Sigma). This resulted in expression of HA-Rab4 in an amount that exceeded endogenous levels by 4- to 5-fold (as determined by quantitative Western blot with a monospecific polyclonal antibody to recombinant Rab4).

Antibodies. Monoclonal antibody (mAb) against the influenza virus HA peptide (M-Q-D-L-P-G-N-D-N-S-T-A-G) was used for epitope tagging (P.v.d.S., M. Ittensohn, and I.M., unpublished work). The mAbs against CHO lgp-B (1:5 crude supernatant), hTfn-R, have been described (12, 21). The affinity-purified rabbit antibody to rat Cbvn (MC9) was also described and was the generous gift of Pietro De Camilli (20) (Yale University).

Fluorescein Isothiocyanate (FITC)-Tfn Pulse-Chase Studies. Cells expressing HA-Rab4 and myc-hTfn-R were grown on coverslips and preincubated in serum-free medium containing 2 mg/ml BSA and 20 mM Na Hepes (pH 7.4) for 30 min at 37°C, immediately prior to uptake experiments. FITC-conjugated transferrin (FITC-Tfn) (Molecular Probes) was prebound to the cells on ice for a period of 45 min at a concentration of 25–100 μg/ml. Synchronized internalization was initiated by placing the coverslips into prewarmed medium for various periods of time at 37°C. At the end of each time point, the coverslips were rinsed briefly in ice-cold PBS/Ca^{2+}/Mg^{2+}, and fixed with 2.5% paraformaldehyde. For some of the longer chase periods, FITC-Tfn was chased out of the cells in the presence of 10-fold excess of unlabeled holo-Tfn (Sigma). The cells were subsequently processed for double-label immune fluorescence as described above using mouse anti-HA for HA-Rab4 and rabbit anti-Cbvn followed by Texas Red-goat anti-mouse and cy5-goat anti-rabbit secondary antibodies, respectively. The resulting triple-labeled cells were analyzed by confocal microscopy. Images were merged and aligned using Adobe Photoshop (Adobe Systems, Mountain View, CA). To rule out any bleed-through or cross-talk of the three fluorescent labels with the three filters used, control coverslips were processed for single label and each was examined applying each of the three filters using the same microscope settings as in the triple-labeled conditions.

Scanning Laser Confocal Immunofluorescence Microscopy. Cells were fixed in 2.5% paraformaldehyde and quenched in 50 mM NH_4Cl/PBS (pH 7.4) for 10 min. Cells were then permeabilized and blocked for 1 hr in 0.03% saponin/3% BSA/PBS (blocking buffer) and subsequently incubated for 1 hr with mixtures of primary antibodies in blocking buffer. The coverslips were washed for 1 hr in blocking buffer and counterstained for 30 min with fluorescently labeled secondary antibodies (Jackson ImmunoResearch) at 1:50 dilutions in blocking buffer. The coverslips were then washed in blocking buffer for 30 min with several buffer changes, rinsed in briefly in PBS and then water, and finally mounted in Moviol containing 2.5% 1,4-diazabicyclo[2.2.2]octane (Sigma). The cells were examined with a Bio-Rad MRC 600 confocal microscope attached to a Zeiss Axiovert microscope using separate filters for each fluorochrome viewed (FITC: L_{ex} = 488 nm, L_{em} = 515 LP; Texas Red: L_{ex} = 568 nm, L_e = 585 LP; and cy5: L_{ex} = 647 nm, L_{em} = 680). Control slides (single labeled with each primary/secondary combination) were examined to ensure that no cross-talk or bleed-through occurred for the given confocal conditions. Primary and secondary antibody crossreactivity was also ruled out.

Drug Treatments. Cells were incubated in medium as described above containing either nocodazole (30 μM), brefeldin A (BFA, 20 μM), or taxol (20 μM) before, during, or after FITC-Tfn internalization as described in the *Results*.

Image Quantitation. The National Institutes of Health Image analysis program was used to quantify the relative number of structures that contained FITC-Tfn, with or without HA-Rab4. Structures positive for FITC-Tfn and negative for HA-Rab4 were detected as green in two channel red–green merged images. To calculate the amount of green only, the red channel was subtracted from the green channel after careful manual alignment. The green pixel area was then measured and expressed as a percentage of total fluorescence. This was performed over a wide range of pixel intensities for both the red and green channels to control for the relative contributions of pixel intensity bias.

RESULTS

Kinetics of FITC-Tfn Translocation from the Cell Periphery to Perinuclear Recycling Endosomes. Tfn was followed in 0.75-μm confocal sections as it moved through the endosomal pathway after the endocytosis of FITC-conjugated Tfn prebound in the cold to plasma membrane Tfn receptors. Confocal microscopy was necessary because the populations of vesicles labeled were found to vary in three dimensions. All focal planes were examined at various times of internalization to visualize the maximum amount of Tfn at each time point.

As shown in Fig. 1*a* (top left panel), FITC-labeled Tfn bound to the cell surface at 0°C gave a uniformly distributed punctate pattern reflecting localization of the ligand on the plasma membrane and in plasma membrane coated pits. The focal plane shown is from the mid-section of the cell to the adherent surface. After brief internalization by warming for 1 min, the Tfn began to move inward, and was found in punctate endosomal structures present at the cell periphery. Again, the focal plane includes the adherent surface of the cell. Thus, many endosomes that appear to be in the center of the cell are actually internal to the adherent cell surface and beneath the centrally located cell nuclei. After 5 min of internalization, FITC-Tfn began to accumulate in crescent-like clusters next to the nucleus in a focal plane extending down from the top of the nucleus. By 15 min, remaining intracellular Tfn had begun to exit from the perinuclear vesicles and to accumulate in a population of endosomal structures found over the nucleus. The focal plane shown extends from the mid-section of the cell, through and above the nucleus. At this 15-min time point, little additional Tfn labeling was detected in optical sections closer to the adherent surface (not shown) (as were used for the other three panels). At times greater than 15 min, the amount of intracellular FITC-Tfn decreased markedly and, in the presence of unlabeled ligand, was completely chased from the cells (not shown).

The perinuclear accumulation of Tfn-containing endosomes is characteristic of the previously described population of vesicles found close to the MTOC and thought to represent a distinct RV or recycling endosome compartment (4–9). Because RVs have not been found to possess any distinguishing biochemical features, they are most often defined solely by their distribution within the cell using conventional fluorescence microscopy. Confocal microscopy revealed, however, that perinuclear Tfn-containing endosomes actually consisted of at least two populations, vesicles lateral vs. vesicles dorsal to the nucleus, labeled at early and late times of chase, respectively.

Importantly, the RV population was clearly distinct from other organelles found in the perinuclear region based on double-label immunofluorescence using antibodies to lgp-B

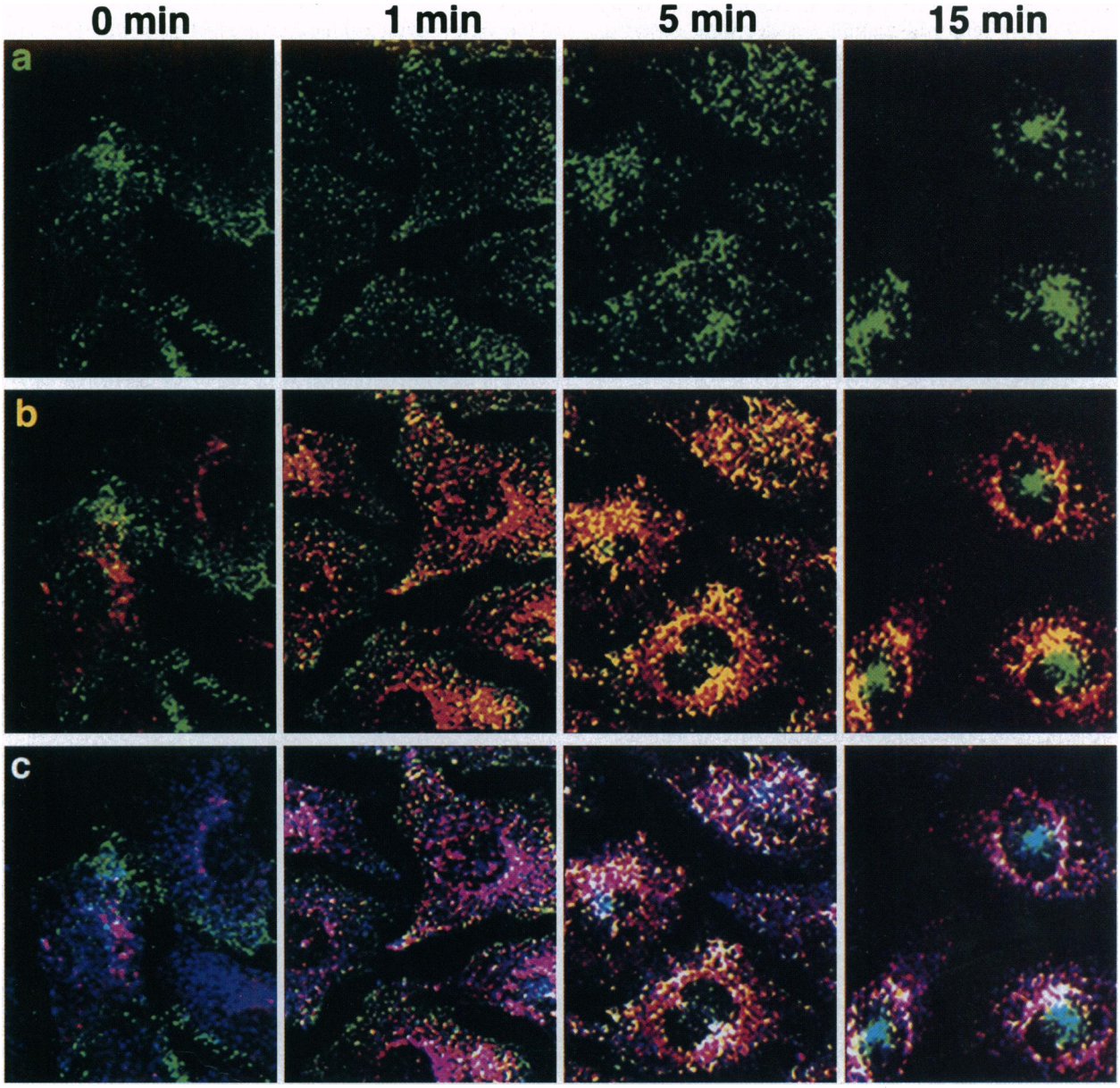

FIG. 1. FITC-Tfn moves from the cell periphery through Rab4-positive endosomes before entering Rab4-negative, Cbvn-positive recycling endosomes. A pulse of FITC-Tfn was followed for various times of chase as described. At each time point, cells were fixed and processed for immunofluorescence to visualize Rab4 and Cbvn. The resulting triple-labeled cells were examined by confocal microscopy. (*a*) As seen in the top four panels the green Tfn is first viewed in the cell periphery between 0 and 1 min of chase, and then moves inward toward the perinuclear region after 5 min, and finally accumulates at the MTOC after 15 min. (*b*) The same cells as in *a* are now shown viewing both the FITC-Tfn (green) channels and the HA-Rab4 (red) channels. Regions of overlap appear as yellow. After 1 min there was little colocalization between FITC-Tfn and HA-Rab4, whereas at 5 min, the colocalization was extensive and most pronounced. After 15 min, most of the FITC-Tfn was found in vesicles over the nucleus, which could only be visualized at optical sections well above the adherent surface. The vesicles above the nucleus were negative for HA-Rab4 and thus appeared green. (*c*) The same cells as in *a* and *b* are shown displaying all three channels: FITC-Tfn (green), HA-Rab4 (red), and Cbvn (blue). Regions of overlap between HA-Rab4 and Tfn appear as yellow, Cbvn as magenta/purple, and Tfn and Cbvn as light blue/aqua. Regions of overlap between all three fluorescent labels appear white. Note that the peripheral FITC-Tfn vesicles are devoid of Rab4 and Cbvn after 1 min. After 5 min, the FITC-Tfn signal is accumulating in white structures adjacent to the nucleus, which contains both Rab4 and Cbvn. By 15 min, much of the Tfn has chased into the vesicles just above the nucleus, which are Cbvn-positive, but Rab4-negative (aqua).

(late endosomes, lysosomes), calnexin (endoplasmic reticulum), and mannosidase II (cis-medial Golgi) and TGN-38 (trans-Golgi network). The RVs were also inaccessible to MPR71040 (L_{ex} = 650, L_{em} = 675) -labeled low density lipoprotein, a receptor-bound ligand that is not recycled, but is transported from early endosomes to late endosomes (not shown).

The cells in Fig. 1*a* were next stained with antibodies to Cbvn and HA-Rab4 to determine if the morphological heterogeneity of endosomes involved in FITC-Tfn transport reflected differences in the distributions of proteins known to regulate Tfn recycling.

Recycling Endosomes Are Rab4 Negative, but Rab4 Is Present on Early Endosomes. Fig. 1*b* contains a series of merged confocal images that illustrate the transit of FITC-Tfn (green) through HA-Rab4 (red)-containing endosomes; structures positive for both markers appear as yellow. At time 0, there is very little overlap between HA-Rab4 and Tfn. Any yellow color is due to the fact that the entire cell surface is uniformly labeled by the FITC-Tfn, which thus "overlaps" with intracellular Rab4-positive structures present in the same optical section. Although >50% of the FITC-Tfn was internalized after 1 min (12), only a small fraction had reached the

red HA-Rab4-positive structures. Distinct populations of single-positive green- and red-staining vesicles were observed, with only a small number of vesicles that were yellow and thus positive for both markers.

By 5 min FITC-Tfn colocalized extensively with HA-Rab4, which is indicated by the large number of yellow structures especially in the perinuclear region. Some Rab4-positive/Tfn-negative (red) endosomes were observed in the cell periphery. By 15 min, the Tfn chased into the RVs above the nucleus and strikingly, most of these structures seemed to lack or be depleted in Rab4. As discussed above, this population was best visualized at 15 min of chase by choosing optical sections well above the adherent cell surface. At 15 min, little additional FITC-Tfn was seen in vesicles, either Rab4-positive or -negative, in optical sections taken at lower planes of focus (not shown). Thus, Tfn seemed to move from the cell periphery into and through a population of Rab4-containing early endosomes before entering RVs above the nucleus that were relatively depleted of Rab4. Although Rab4-positive and -negative structures could be distinguished, they occupy similar perinuclear locations in the cytoplasm.

Both Rab4 and Cbvn Are Present on the Early Endosomes, Whereas only Cbvn Is Found on the Recycling Endosomes. To better monitor the transit of FITC-Tfn through endocytic structures, the cells in Fig. 1 *a* and *b* were also stained for the v-snare, (Cbvn). Fig. 1*c* displays the merge of all three endocytic markers: overlap of HA-Rab4 (red) and FITC-Tfn (green) yielded yellow, whereas overlap of Cbvn (blue) and FITC-Tfn yielded light blue. Codistribution of HA-Rab4 (red) and Cbvn (dark blue) yields purple, whereas regions where all three proteins overlapped appeared white. After 1 min, there was a population of early endocytic vesicles that was labeled by FITC-Tfn (green), but did not contain detectable HA-Rab4 or Cbvn. These single positive Tfn-containing structures may reflect FITC-Tfn still at the cell surface or in clathrin-coated vesicles. Also visible were purple vesicles positive for HA-Rab4 and Cbvn. A few white endosomes containing all three markers were also seen. By 5 min, almost all of the FITC-Tfn could be found in endosomes that contained both HA-Rab4 and Cbvn. These white, triple-positive endosomes were, as expected, largely in the perinuclear cytoplasm.

Strikingly, between 5 and 15 min, much of the internalized FITC-Tfn had exited the white, triple-positive perinuclear structures to accumulate in the RV population above the nucleus, which was positive for Cbvn but negative for Rab4 yielding aqua-colored structures. Thus, RVs can be distinguished from other early endosome populations not only on the basis of their kinetics of labeling with FITC-Tfn and location in the cell, but also on the basis of their biochemical composition, i.e., the presence of Cbvn and the absence of Rab4. The distribution of these two markers on the recycling endosomes was not a manifestation of the pulse-chase conditions, because the same results were obtained in cells that were continuously labeled with FITC-Tfn for 30 min at 37°C (not shown).

We interpret these results to mean that Tfn passes through a population of Rab4- and Cbvn-positive peripheral and perinuclear early endosomes prior to reaching a distinct population of RVs found above the nucleus that contain Cbvn, but are depleted in Rab4.

Nocodazole Does Not Completely Inhibit the Formation of Rab4-Negative Recycling Endosomes. The perinuclear population of Tfn-containing RVs disperses upon treatment with microtubule depolymerizing agents such as nocodazole (8, 22, 23). We next asked whether the more randomly distributed endosomes of nocodazole-treated cells still included a distinct population of Rab4-negative RVs. FITC-Tfn was bound on ice to cell surface receptors in cells that had been pretreated with nocodazole for 60 min. The cells were then warmed to 37°C in the presence of nocodazole for 1–20 min. Parallel cells were processed in the absence of nocodazole, and results similar to those represented in Fig. 1*b* were obtained. Fig. 2 is a merged image of Rab4 (red) and FITC-Tfn (green) fluorescence in which regions of overlap appear as yellow. At early time points (1 min), Tfn was first seen in peripheral, Rab4-negative structures similar to those seen in Fig. 1*a* at 1 min. As in the absence of nocodazole, after 5 min of chase, almost all of the Tfn was found in Rab4-positive structures in the presence of the drug, and in all focal planes examined. After 20 min, the appearance of FITC-Tfn in the characteristic population of Rab4-depleted RVs was only seen in control cells. In nocodazole-treated cells, the Tfn-positive endosomes were far more evenly distributed throughout the cytoplasm. Although there remained a considerable degree of colocalization of FITC-Tfn in Rab-positive structures (yellow) of the nocodazole-treated cells, it was clear that Tfn was also detected in Rab4-negative (green) structures. Quantitation of these images indicated that there were 30–50% fewer Tfn-only containing endosomes in the nocodazole-treated cells as compared with controls. Thus, although nocodazole may have decreased the formation of or transit to a Rab4-depleted RV population, it did not completely inhibit the process.

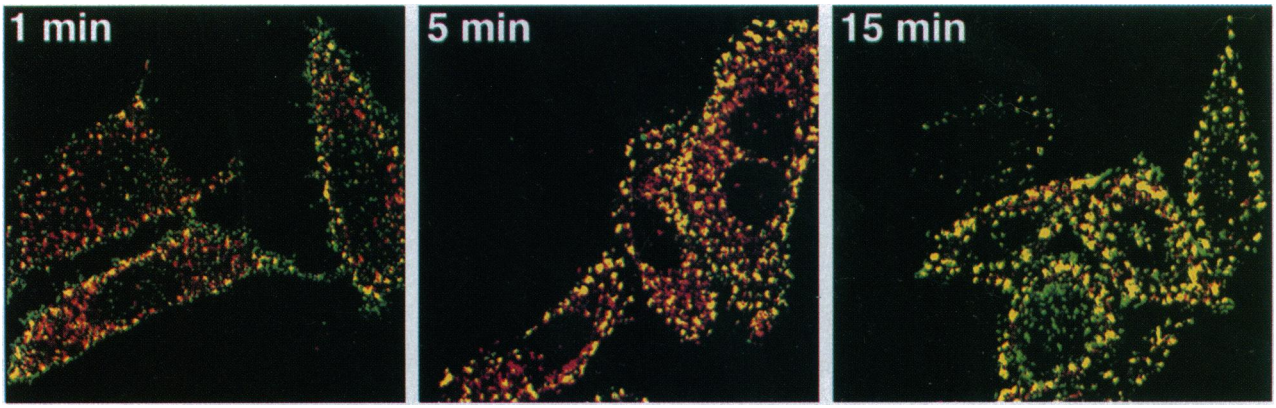

FIG. 2. Nocodazole does not completely inhibit the formation of Rab4-negative recycling endosomes. An FITC-Tfn (green) pulse-chase experiment similar to Fig. 1 was performed in cells that were treated with nocodazole as described in the *Results*, and counterstained for HA-Rab4 (red). Regions of overlap appear as yellow. In early time points, Tfn is first seen to appear in peripheral, Rab4-negative endosomes. After 5 min of chase, the Tfn moves into the Rab4-positive structures, but after 20 min of chase, there is a high degree of colocalization (yellow) of Tfn with Rab4 that persists at this late time point when compared with the untreated cells (see Fig. 1*b*, 15 min). However, the nocodazole-treated cells still maintain some capacity to generate Rab4-negative (green) RVs, although the perinuclear recycling compartment is dispersed by the loss of microtubules.

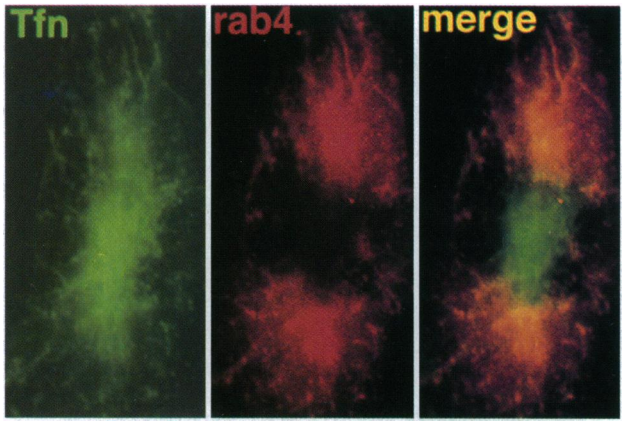

FIG. 3. RVs remain Rab4 negative in the presence of BFA. Cells were treated with BFA and then continuously labeled with FITC-Tfn (green) as described in the *Results*. Following fixation, cells were stained for Rab4 (red), and examined by standard epifluorescence microscopy. Black and white negatives were scanned and processed in Adobe Photoshop. Tfn was present in tubular and vesicular structures in the peripheral cytoplasm, as well as in a dense accumulation of less distinct structures next to and over the nucleus. Staining for HA-Rab4 (red) showed that most of the peripheral Tfn-containing tubular endosomes were also strongly Rab4-positive, but Rab4 was noticeably absent from the RVs above the nucleus.

In control experiments, we confirmed that nocodazole treatment, but not simple incubation of the cells at 0°C in the absence of the drug, was effective at depolymerizing the CHO cell microtubule network. However, when cells were stained for stable microtubules, one or two long microtubules persisted in almost every cell. Thus, the drug effect was likely to reflect at best only a partial requirement for microtubules on RV formation or delivery. Interestingly, the RVs were also dispersed after prolonged exposure to (1 hr) the microtubule-stabilizing agent taxol (not shown), suggesting that dynamic microtubule networks are needed for the localization of RVs to the perinuclear region.

RVs Remain Rab4 Negative in the Presence of BFA. Treatment of cells with the fungal metabolite BFA has been documented to cause the tubulation and fusion of various organelles including endosomes (22, 24–26). To determine if the Rab4-negative perinuclear RVs remain distinct from Rab4-positive early endosome elements upon BFA treatment, cells were pretreated for 15 min with BFA and then continuously labeled with FITC-Tfn for 15 min at 37°C in the continued presence of the drug. As shown in Fig. 3, FITC-Tfn (green) was present in tubular and vesicular structures in the peripheral cytoplasm, as well as in a dense accumulation of less distinct structures next to and over the nucleus. Staining for HA-Rab4 (red) showed that most of the peripheral Tfn-containing endosomes were also strongly Rab4-positive; however, Rab4 was absent from the perinuclear endosomes. Identical results were obtained when the cells were first labeled with Tfn and then treated with BFA. Thus, even in the presence of a drug that dramatically alters endosomal morphology and is known to cause the redistribution of endosomal markers to another compartment (trans-Golgi network), a population of Rab4-negative RVs remained. This provides further support for our observation that Rab4-positive early endosomes and the Rab4-negative RVs are distinct.

DISCUSSION

The intracellular pathway of Tfn endocytosis and recycling has been extensively studied in a variety of mammalian cell types (2). A common observation is that some or all of the internalized receptors transiently accumulate in vesicles and tubules near the MTOC. This is particularly evident in the case of Tfn receptor (5, 6). On the basis of electron microscopy, as well as the inefficiency at which internalized Tfn receptors reach sialyl transferase-containing compartments (27, 28), these vesicles are thought to be distinct from the trans-Golgi network and have been proposed to represent a "compartment" of RVs (4–8). This idea has received support from the finding that forms of crosslinked Tfn, which are not transported to lysosomes, appear to be transiently retained in the RV population (10). Fluorescence microscopy has also suggested that there may be retrograde transport from RVs back to more peripheral early or sorting endosomes (9).

Because RVs have yet to be characterized in terms of possible intrinsic markers, it has been impossible to determine whether they are biochemically distinct from the early endosomes from which they receive their contents much less whether RVs comprise a bona fide compartment. The lack of intrinsic markers has also limited analysis of RV function *in vitro* or even in intact cells because their identification is typically dependent on their characteristic perinuclear distribution. In cell types other than CHO cells, even this pathognomonic distribution is often less than clear, suggesting that RVs do not always exist, or that they can be more widely distributed throughout the cytoplasm.

By analyzing the distribution of two endogenous membrane-associated proteins known to play functionally important roles in Tfn receptor recycling, we have now been able to establish at least one biochemical feature that distinguishes RVs from other common early endosomal elements. Although the absence of a marker, in this case Rab4, is not as satisfying as would be the identification of a component that is selectively enriched in RVs, it nevertheless provides a piece of direct evidence—as well as the first ligand-independent criterion—to describe RVs as distinct entities. The absence of Rab4 from RVs thus enables us to distinguish between early endosomes and RVs. Operationally, we now define early endosomes as that population of peripheral and/or perinuclear structures that are both Rab4 and Cbvn positive, and that are reached by incoming ligands shortly after internalization. RVs, on the other hand, represent an Rab4-depleted endosome population in which at least some recycling receptors accumulate prior to their return to the plasma membrane. Because dissociated ligands rarely if ever appear in RVs (9), it is clear that receptor-ligand dissociation and sorting generally occurs in early endosomes, or at least prior to receptor arrival in RVs. It is important to note that not all vesicles in the perinuclear region are equivalent, i.e., Rab4-positive and -negative vesicles are present in roughly the same region.

It has now become important to resolve several issues concerning the nature and function of RVs. First, the actual fraction of any one recycling receptor that passes through RVs must be determined. Although it is possible that all Tfn receptors reach RVs as an obligatory intermediate on the recycling pathway, we cannot rule out the possibility that some or even a large fraction of receptor recycles to the cell surface directly from early endosomes, avoiding transit through RVs. The existence of such a "short circuit" may explain why FITC-Tfn seems to persist in RVs for times somewhat longer than the $t_{1/2}$ of Tfn recycling measured biochemically. The asynchrony of receptor transport during endocytosis, as well as inherent differences between biochemical and fluorescence measurements, are more likely explanations, but the obligatory nature of RVs must be established directly.

In this respect, the absence of Rab4 from RVs is also interesting. Conceivably, Rab4 is required for the fusion of early endosome-derived transport vesicles with RVs. Rapid dissociation of Rab4 from the RV membrane following the hydrolysis of Rab4-bound GTP may explain its absence from the putative target. It is also possible, however, that Rab4 mediates the fusion of early endosome-derived transport ves-

icles with the plasma membrane; thus, Rab4 is not found on RVs because it is not involved in their function but rather in the short circuit back from early endosomes to the plasma membrane. Such a mechanism would predict that RVs will be associated with another member of the Rab protein family. Earlier findings that overexpression of Rab4 in CHO cells results in the redistribution of Tfn receptors from intracellular membranes to the cell surface would be consistent with either possibility (12).

Direct fusion is supported by suggestions that endosome-derived vesicles carrying the insulin-regulated glucose transporter (Glut4) appear to be Rab4-positive, and that Rab4 may be involved in Glut4 recruitment to the plasma membrane in response to insulin stimulation (reviewed in ref. 29). Identification of the possible fusion step under the control of Rab4, as well as identification of RV-associated Rab proteins, will represent important next steps in resolving this issue. A similar situation exists for the step(s) controlled by Cbvn. Although apparently not involved in homotypic endosome–endosome fusion (29), it does appear that Cbvn is required for Tfn to complete its cycle based on the sensitivity of Cbvn and Tfn recycling to botulinum toxin in permeabilized CHO cells (20).

Perhaps most intriguing of all is why RVs, at least in some cells, exhibit a characteristic distribution closely associated with the MTOC. It is not immediately obvious why some or all recycling receptors must transit to the perinuclear cytoplasm before returning to the cell surface. Although microtubule antagonists (nocodazole, taxol) interfere with the ability of FITC-Tfn to reach Rab4-negative RVs, it is clear that intact and functional microtubule networks are not absolutely required. Similarly, the fact that Tfn receptor recycling is not dependent on microtubules (22, 23, 31) indicates that there is no obligatory reason to reach the perinuclear cytoplasm to recycle.

One likely explanation for the positioning of RVs near the MTOC comes from a consideration of polarized epithelial cells, rather than from the relatively nonpolarized CHO cells. In epithelial cells, vesicle transport from the basolateral to the apical cytoplasm is strongly dependent on microtubules. Disruption of microtubule networks with nocodazole or colchicine severely inhibits basolateral to apical transcytosis in MDCK and other cells (32). Moreover, even recycling markers internalized at the basolateral surface appear to accumulate on the apical side of the nucleus in MDCK cells, at a site close to the MTOC (33, 34). Translocation of all vesicles derived from basolateral early endosomes to the apical cytoplasm would allow all vesicle populations equal access to both the apical and basolateral plasma membranes. It would also provide the opportunity for all recycling receptors, regardless of whether they were internalized apically or basolaterally, to reach a common intracellular site where fusion or additional receptor sorting events relevant to bi-directional transcytosis might thus occur.

Irrespective of how these issues are resolved, our work has established a biochemical basis from which to proceed, namely that RVs can now be independently distinguished from other early endosomal elements.

We would like to thank Pietro De Camilli and the members of the Mellman–Hellenius group for many valuable discussions. Michael Nathanson and Philippe Male provided invaluable training and assistance at the confocal microscope at the Yale Cell Biology Center for Cell Imaging. We also thank John Presley and Beate Sodeik for insights, discussions, and technical advice. Molecular Probes generously provided the MPR71040 labeled low density lipoprotein. This work was supported by grants from the National Institutes of Health (to I.M.), the Donaghue Medical Research Foundation, the Netherlands Diabetes Foundation, and the Royal Netherlands Academy of Arts and Sciences (to P.v.d.S.). E.D. is supported by a Miles/Bayer Predoctoral Scholar Award.

1. Steinman, R. M., Mellman, I., Muller, W. A. & Cohn, Z. A. (1983) *J. Cell Biol.* **96,** 1–27.
2. Trowbridge, I. S., Collwan, J. F. & Hopkins, C. R. (1993) *Annu. Rev. Cell Biol.* **9,** 129–162.
3. Geuze, H. J., Slot, J. W. & Schwartz, A. L. (1987) *J. Cell Biol.* **104,** 1715–1723.
4. McGraw, T. E., Greenfield, L. & Maxfield, F. R. (1987) *J. Cell Biol.* **105,** 207–214.
5. Hopkins, C. R. & Trowbridge, I. S. (1983) *J. Cell Biol.* **97,** 508–521.
6. Yamashiro, D. J., Tycko, B., Fluss, S. R. & Maxfield, F. R. (1984) *Cell* **37,** 789–800.
7. Hopkins, C. R., Gibson, A., Shipman, M. & Miller, K. (1990) *Nature (London)* **346,** 335–339.
8. Tooze, J. & Hollinshead, M. (1991) *J. Cell Biol.* **115,** 635–653.
9. Ghosh, R. N. & Maxfield, F. R. (1995) *J. Cell Biol.* **128,** 549–562.
10. Marsh, E. W., Leopold, P. L., Jones, N. L. & Maxfield, F. R. (1995) *J. Cell Biol.* **129,** 1509–1522.
11. Zerial, H. & Stenmark, H. (1993) *Curr. Opin. Cell Biol.* **5,** 613–620.
12. van der Sluijs, P., Hull, M., Webster, P., Goud, B. & Mellman, I. (1992) *Cell* **70,** 729–740.
13. Bucci, C., Parton, R., Mather, I., Stunnenberg, H., Simons, K. & Zerial, M. (1992) *Cell* **70,** 715–728.
14. Chavrier, P., Parton, R. G., Hauri, H. P., Simons, K. & Zerial, M. (1990) *Cell* **62,** 317–329.
15. Lombardi, D., Soldati, T., Riederer, M., Zerial, M. & Pfeffer, S. (1993) *EMBO J.* **12,** 677–682.
16. Gorvel, J. P., Chavrier, P., Zerial, M. & Gruenberg, J. (1991) *Cell* **64,** 915–925.
17. Sollner, T., Whiteheart, S., Brunner, M., Bromage, H., Geromanos, S., Tempst, P. & Rothman, J. E. (1993) *Nature (London)* **362,** 318–323.
18. Bennett, M. K. & Scheller, R. H. (1994) *Annu. Rev. Biochem.* **63,** 63–100.
19. McMahon, H. T., Ushkayov, Y. A., Edelmann, L., Link, E., Binz, T., Niemann, H., Jahn, R. & Sudhof, T. C. (1993) *Nature (London)* **364,** 346–349.
20. Galli, T., Chilcote, T., Mundigl, O., Binz, T., Niemann, H. & DeCamilli, P. (1994) *J. Cell Biol.* **125,** 1015–1024.
21. Evan, G. I., Lewis, G. K., Ramsay, G. & Bishop, J. M. (1985) *Mol. Cell. Biol.* **5,** 3610–3616.
22. McGraw, T. E., Dunn, K. W. & Maxfield, F. R. (1993) *J. Cell. Physiol.* **155,** 579–594.
23. Sakai, T., Yamashina, S. & Ohnishi, S. (1991) *J. Biochem. (Tokyo)* **109,** 528–533.
24. Hunziker, W., Whitney, J. A. & Mellman, I. (1991) *Cell* **67,** 617–627.
25. Lippincott-Schwartz, J., Yuan, L., Tipper, C., Amherdt, M., Orci, L. & Klausner, R. D. (1991) *Cell* **67,** 601–616.
26. Wood, S. A., Park, J. E. & Brown, W. J. (1991) *Cell* **67,** 591–600.
27. Snider, M. D. & Rogers, O. C. (1985) *J. Cell Biol.* **100,** 826–834.
28. Volz, B., Orberger, G., Porwoll, S., Hauri, H. P. & Tauber, R. (1995) *J. Cell Biol.* **130,** 537–551.
29. James, D. E., Piper, R. C. & Slot, J. W. (1994) *Trends Cell Biol.* **4,** 120–126.
30. Link, E., McMahon, H., Fischer von Mollard, G., Yamasaki, S., Niemann, H., Sudhof, T. C. & Jahn, R. (1993) *J. Biol. Chem.* **268,** 18423–18426.
31. Jin, M. & Snider, M. D. (1993) *J. Biol. Chem.* **268,** 18390–18397.
32. Hunziker, W., Male, P. & Mellman, I. (1990) *EMBO J.* **9,** 3515–3525.
33. Apodaca, G., Katz, L. A. & Mostov, K. E. (1994) *J. Cell Biol.* **125,** 67–86.
34. Barroso, M. & Sztul, E. S. (1994) *J. Cell Biol.* **124,** 83–100.